Experimental Investigation of the Anisotropic Thermal Conductivity of C/SiC Composite Thin Slab

Ke-Fan Wu(毋克凡)[1], Hu Zhang(张虎)[1*], and Gui-Hua Tang(唐桂华)[2]

[1]*State Key Laboratory for Strength and Vibration of Mechanical Structures, School of Aerospace Engineering, Xi'an Jiaotong University, Xi'an 710049, China*

[2]*MOE Key Laboratory of Thermo-Fluid Science and Engineering, School of Energy and Power Engineering, Xi'an Jiaotong University, Xi'an 710049, China*

(Received 31 December 2023; accepted manuscript online 28 February 2024)

Fiber-reinforced composites possess anisotropic mechanical and heat transfer properties due to their anisotropic fibers and structure distribution. In C/SiC composites, the out-of-plane thermal conductivity has mainly been studied, whereas the in-plane thermal conductivity has received less attention due to their limited thickness. In this study, the slab module of a transient plane source method is adopted to measure the in-plane thermal conductivity of a 2D plain woven C/SiC composite slab, and the test uncertainty is analyzed numerically. The numerical investigation proves that the slab module is reliable for measuring the isotropic and anisotropic slabs with in-plane thermal conductivity greater than 10 $\mathrm{W{\cdot}m^{-1}{\cdot}K^{-1}}$. The anisotropic thermal conductivity of the 2D plain woven C/SiC composite slab is obtained within the temperature range of 20–900 ℃ by combining with a laser flash analysis method to measure the out-of-plane thermal conductivity. The results demonstrate that the out-of-plane thermal conductivity of C/SiC composite decreases with temperature, while its in-plane thermal conductivity first increases with temperature and then decreases, and the ratio of in-plane thermal conductivity to out-of-plane thermal conductivity is within 2.2–3.1.

DOI: 10.1088/0256-307X/41/3/034401

1. Introduction. Although ceramic materials have the advantages of high strength, hardness and temperature resistance, their application is limited because of their brittleness and structural defects. Continuous fibers are usually introduced as reinforcement to improve the comprehensive performance of polymer and ceramic materials.[1–3] Carbon fiber-reinforced SiC matrix (C/SiC) composites combine the benefits of carbon fiber and a SiC matrix, which can be applied in thermal protection fields, such as in supersonic aircraft, rocket engines, nuclear reactors and gas turbines.[4–6]

There are many SiC matrix composite manufacturing methods, such as liquid silicon infiltration,[7] polymer impregnation pyrolysis,[8] chemical vapor infiltration (CVI),[6] and reactive melt infiltration.[9] Among them, the CVI method is widely used in the manufacture of C/SiC composites. Due to the anisotropic physical characteristics of carbon fibers and the directional woven structure of preforms, C/SiC composites have anisotropy in both mechanical and thermal properties.[10–14] According to the woven method of fibers, the woven types of C/SiC composites include 2D plain woven, 3D orthogonal woven, and 3D needled structure types.[1,15] The heat transfer along the carbon fiber is several times greater than that perpendicular to it,[16–18] while the SiC matrix is isotropic. In addition, the in-plane thermal conductivity $\lambda_{\text{in-plane}}$ is higher than the out-of-plane thermal conductivity $\lambda_{\text{out-of-plane}}$ in 2D plain woven C/SiC composite because the fibers are distributed orthogonally in the plane.

Thermal conductivity λ is essential for evaluating the heat transfer performance of composites.[19,20] Many works have been conducted to predict the anisotropic thermal conductivity $\lambda_{\text{anisotropic}}$ of C/SiC composites numerically,[21–24] and yet the corresponding experimental studies at high temperature are rarely reported. For the studies of the measurement of the $\lambda_{\text{out-of-plane}}$, Zhang *et al.*[11,12] obtained the out-of-plane thermal diffusivity $a_{\text{out-of-plane}}$ of 2D plain woven C/SiC composite using a laser flash analysis (LFA) method within the temperature range of 100–500 ℃. Cai *et al.*[13] measured the $a_{\text{out-of-plane}}$ of 3D C/SiC composite over a temperature range from 25 ℃ to 1300 ℃ by adopting the LFA method, and the $\lambda_{\text{out-of-plane}}$ was obtained by measuring its specific heat capacity and density simultaneously. Xu *et al.*[14] studied the $\lambda_{\text{in-plane}}$ and $\lambda_{\text{out-of-plane}}$ of 2D plain woven C/SiC composite using a transient plane source (TPS) method within the temperature range of 27–800 ℃ for comparison with numerical results. However, the test uncertainty associated with measuring the $\lambda_{\text{anisotropic}}$ of C/SiC composites with the TPS method was not analyzed. In C/SiC composites, the $\lambda_{\text{in-plane}}$ is also crucial for the design of the thermal protection system. A higher $\lambda_{\text{in-plane}}$ could improve the ability of heat transfer in the in-plane direction, resulting in a lower temperature at the hot spot.

*Corresponding author. Email: huzhang@xjtu.edu.cn

© 2024 Chinese Physical Society and IOP Publishing Ltd

Many methods for measuring the $\lambda_{\text{in-plane}}$ are constrained by the limited thickness of C/SiC composites caused by the manufacturing process. When adopting the steady-state method, the ideal 1D heat conduction should be satisfied within the test sample, which requires the length of the test sample to be much larger than its thickness. In comparison, the transient methods offer a shorter test time and a wider thermal conductivity test range. The planar λ vertical to the wire/strip orientation can be measured via one single measurement using the transient hot wire/strip method, and the $\lambda_{\text{anisotropic}}$ can be obtained by switching the measurement direction, which is also subjected to the very finite thickness of C/SiC composites. In addition, the hot wire/strip method is unsuitable for measuring high conductive materials.[25] The TPS method has been adopted to measure the thermal conductivity of bulk isotropic/anisotropic medium and thin slabs.[26–28] The $\lambda_{\text{in-plane}}$ and $\lambda_{\text{out-of-plane}}$ of an orthotropic medium with known volumetric heat capacity can be determined using the TPS method via one single test. In anisotropic thin slabs, their $\lambda_{\text{in-plane}}$ can be measured using the slab module of the TPS method, which assumes that the outer surface of the test slab is ideally thermally insulated. However, the heat released from the sensor will dissipate to the outer background thermal insulation material, which affects the test reliability.

In this Letter, the uncertainty of applying the TPS slab module to both isotropic and anisotropic slabs is analyzed quantitatively via numerical simulation, and the influence of different background thermal insulation materials on test uncertainty is also discussed. Experiments are also conducted to verify the numerical results. Then, the TPS slab module is adopted to measure the $\lambda_{\text{in-plane}}$ of 2D plain woven C/SiC composite within the temperature range of 20–900 ℃. Meanwhile, the corresponding temperature-dependent $\lambda_{\text{out-of-plane}}$ is obtained using the LFA method.

2. Experimental Method.

2.1. Test Material. The 2D plain woven C/SiC composite manufactured using the CVI method has a density of 2.1 g·cm^{-3}. Figure 1 presents the surface morphology and microstructure observed using a scanning electron microscope (SEM) (SU3500, Tianmei, China). The fiber bundles are orthogonally distributed, and the volume fraction of the fiber is 50%.

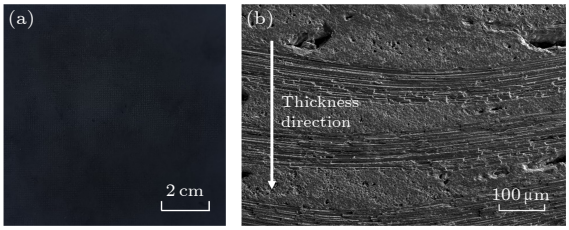

Fig. 1. Surface morphology (a) and SEM (b) of the 2D plain woven C/SiC composite.

2.2. TPS Method for Measuring In-Plane Thermal Conductivity. As displayed in Fig. S1 of the Supplementary Materials, the test sensor, which serves as both a heating element and temperature sensor in TPS measurement, is placed between two identical thin slabs. The thermal insulation material with lower λ is applied to the outer face of the test slab to minimize the heat dissipation. Under constant heating, the temperature rise of the sensor is shown in Eq. (1), and the $\lambda_{\text{in-plane}}$ of the test slab can be obtained from the transient sensor temperature response[28]

$$\Delta T(\tau) = \frac{P}{\pi^{3/2} r \lambda_{\text{in-plane}}} E(\tau), \tag{1}$$

where P is the heating power, r is the radius of the sensor, $\lambda_{\text{in-plane}}$ is the in-plane thermal conductivity of the test sample, and $E(\tau)$ is the dimensionless time function.

The $\lambda_{\text{in-plane}}$ of 2D plain woven C/SiC composite is measured with a TPS2500S thermal constant analyzer (Hot Disk, Sweden) in the temperature range of 20 ℃ to 900 ℃. As shown in Fig. S1, a mica 4921 sensor (radius: 9.719 mm) is adopted. The dimensions of the C/SiC composite specimen are 51 mm × 51 mm × 3.18 mm. The background thermal insulation material used at elevated temperature is aluminum silicate fiberboard with thermal conductivity of 0.06 W·m^{-1}·K^{-1} at 20 ℃ and a density of 0.31 g·cm^{-3}. The test slab and sensor are placed in the tubular furnace (ESTF110, Entech, Sweden) and heated to the test temperature in the nitrogen atmosphere.

The background thermal insulation material used in practical measurements is not an ideal adiabatic material, which would affect the test reliability. As presented in Fig. S2 of the Supplementary Materials, four thermal insulation materials are used as the background materials in the $\lambda_{\text{in-plane}}$ measurement of isotropic stainless steel, aluminum, and anisotropic C/SiC composite slab for comparison. The density and thermal conductivity measured at room temperature are also marked in Fig. S2.

2.3. LFA Method for Measuring Out-of-plane Thermal Conductivity. The LFA method is adopted to measure the thermal diffusivity a of the specimen via one single test by using a pulse laser that heats the front surface of the sample and by monitoring the temperature response at the rear surface. With the measured specific heat capacity c_{p} and density ρ, the λ along the sample test direction can be obtained by $\lambda = a \cdot \rho \cdot c_{\text{p}}$.[29]

The LFA467 (NETZSCH, Germany) was adopted to measure the $a_{\text{out-of-plane}}$ of 2D plain woven C/SiC composite within the temperature ranges from 150 ℃ to 900 ℃. The STA449F3 simultaneous thermal analyzer (STA) (NETZSCH, Germany) was employed to measure the temperature-dependent specific heat capacity.

3. Numerical Method. To evaluate the effects of thermal insulation materials on the test uncertainty associated with applying the TPS slab module, numerical analysis is carried out to mimic the transient heat transfer process in a measuring slab with known thermal properties.[26] As presented in Fig. S3 of the Supplementary Materials, two kinds of simulations are carried out. One simulation sets the outer surface of the slab as the adiabatic condition, while the other uses the practical thermal insu-

lation material as background material. The $\lambda_{\text{in-plane}}$ of the slab specimen is determined in reverse from the sensor temperature response with a self-developed program.[26] If the $\lambda_{1\text{-in-plane}}$ that is obtained from adiabatic assumption is identical to the given value $\lambda_{0\text{-in-plane}}$, the reliability of the simulation method can be verified. Furthermore, the $\lambda_{2\text{-in-plane}}$ that is obtained by considering the practical thermal insulation material is compared with the $\lambda_{0\text{-in-plane}}$. Then, the quantitative influence of the thermal conductivity of the thermal insulation material (λ_{TIM}) on the measurement of the slab module of the TPS method can be obtained.

Due to the axisymmetric structure of the TPS sensor, the 3D computation domain is simplified to a 2D domain in the simulation, which is displayed in Fig. S4. The computational domain is further simplified by applying symmetric boundary conditions. Zones 1–4 in the numerical model are the heating element of nickel, mica insulation layer, slab specimen, and background thermal insulation material, respectively. The details of the sensor components are given in Ref. [26]. The mesh grid of the numerical model is determined to be 580800 after mesh independence verification. In the simulations, the time step is 0.001 s, and the convergence criterion of the energy equation is 10^{-10}.

As presented in Fig. S4, the left wall of the computational model is the axis of symmetry, and the down wall is the symmetry boundary. Because the distance from the test slab to the external boundary of the simulation domain is larger than the probing depth of heat within the thermal insulation material and slab specimen, the outer walls of both the thermal insulation material and the slab specimen are set to be adiabatic.

The isotropic and anisotropic materials with different thermal conductivities are selected as the slab specimen in the simulation to verify the test accuracy of the application of the TPS slab module to different slab materials. Tables S1 and S2 in the Supplementary Materials list the input thermal properties of studied isotropic and anisotropic materials. In anisotropic fiber-reinforced composites, the anisotropic ratio of $\lambda_{\text{in-plane}}$ to $\lambda_{\text{out-of-plane}}$ is usually between 1.5 and 4.[14,16,17,22] By fixing the $\lambda_{\text{in-plane}}$, the $\lambda_{\text{out-of-plane}}$ is varied to analyze the influence of the anisotropic ratio on the slab module measurement. For the experimental materials, such as stainless steel, aluminum and C/SiC composite, numerical analysis is also performed to compare with the experimental results, and the thermal properties are displayed in Table S3.

4. Results and Discussion.

4.1 Influence of Thermal Insulation Materials. To analyze the measurement uncertainty caused by the inconsistency between the practical boundary conditions and theoretical adiabatic assumption, both simulation and experiments are performed. First, the outer surface of the slab sample is set as an adiabatic boundary in the simulation, as displayed in Fig. S5. The calculated $\lambda_{\text{in-plane}}$ of different isotropic and anisotropic materials is compared to the given value. For the isotropic materials, the maximum deviation of the calculated λ is 0.43%. Meanwhile, the maximum deviation of the calculated $\lambda_{\text{in-plane}}$ is 0.74% for the anisotropic materials, which indicates that the anisotropic ratio has little effect on the results under the theoretical assumption. The above results prove that the numerical simulation of the TPS slab module is reliable.

Then, the heat transfer processes of practical experiments are reproduced by considering the background thermal insulation materials. By changing λ_{TIM}, the effects of different background materials on the slab specimen measurement are revealed. Taking the C/SiC composite as an example, the temperature distribution and increase in the curve obtained by using different thermal insulation materials are shown in Figs. S6 and S7 of the Supplementary Materials. The results show that more heat dissipates into the background thermal insulation material as λ_{TIM} increases. As a consequence, the total temperature increase curve of the sensor decreases accordingly.

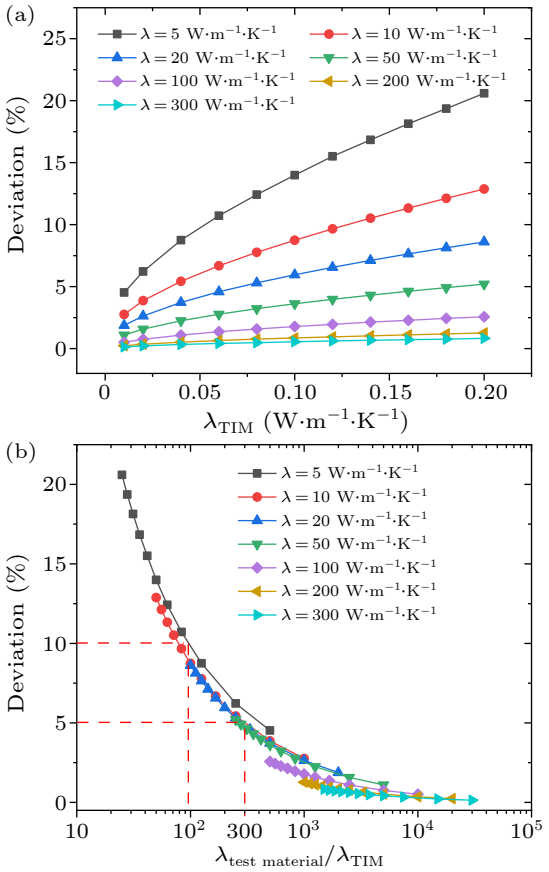

Fig. 2. Deviation in measurements of different isotropic materials (a) versus thermal conductivity of thermal insulation material (λ_{TIM}) and (b) versus $\lambda_{\text{test material}}/\lambda_{\text{TIM}}$.

Figure 2(a) illustrates the deviation of the calculated $\lambda_{\text{in-plane}}$ for different isotropic slab specimens, which increases with λ_{TIM}. The physical explanation for this is that, with the reduction of the thermal insulation ability of the background material, the heat loss increases accordingly, which is deviating from the theoretical assumption. Thus, the measured $\lambda_{\text{in-plane}}$ of the test slab deviates from the real value. The maximum deviation reaches 20.1% in the material with $\lambda = 5\,\text{W}\cdot\text{m}^{-1}\cdot\text{K}^{-1}$.

The deviation decreases as the thermal conductivity of the test material ($\lambda_{\text{test material}}$) increases. If the λ_{TIM} is below $0.1\,\text{W}\cdot\text{m}^{-1}\cdot\text{K}^{-1}$, the test uncertainty will be less than 10% for the slab with $\lambda > 10\,\text{W}\cdot\text{m}^{-1}\cdot\text{K}^{-1}$, which proves that the slab module of the TPS method is reliable for measuring isotropic material with thermal conductivity higher than $10\,\text{W}\cdot\text{m}^{-1}\cdot\text{K}^{-1}$. The ratio of heat diffused into the background thermal insulation material will decrease as the λ_{TIM} decreases or the $\lambda_{\text{test material}}$ increases. To further illustrate the effect of the heat dissipation ratio on the test results, Fig. 2(b) shows the deviation in the measuring slab specimen with different thermal conductivity ratios of test specimen to thermal insulation material. It clearly shows that as the thermal conductivity ratio increases, the ratio of heat diffused into the background thermal insulation material decreases, and the deviation decreases rapidly. If the $\lambda_{\text{test material}}$ is 100 times that of the background material, the deviation caused by non-ideal adiabatic boundary conditions will be less than 10%. For the thermal conductivity ratio of 300, the deviation can be reduced to 5%.

In the anisotropic slab materials, the different anisotropic ratio is investigated by varying the $\lambda_{\text{out-of-plane}}$ and fixing the $\lambda_{\text{in-plane}}$. Meanwhile, the λ_{TIM} is fixed at $0.1\,\text{W}\cdot\text{m}^{-1}\cdot\text{K}^{-1}$. The deviation between the calculated $\lambda_{\text{in-plane}}$ and input value is displayed in Fig. 3. With the increment of the anisotropic ratio, the deviation increases slowly and the difference between the isotropic case and anisotropic cases is less than 1.3%. The simulation results show that the anisotropic ratio of the material has a less and negligible influence on the measurement of the slab module. The above results can be applied to guide the users on how to prepare the TPS slab test with an acceptable accuracy.

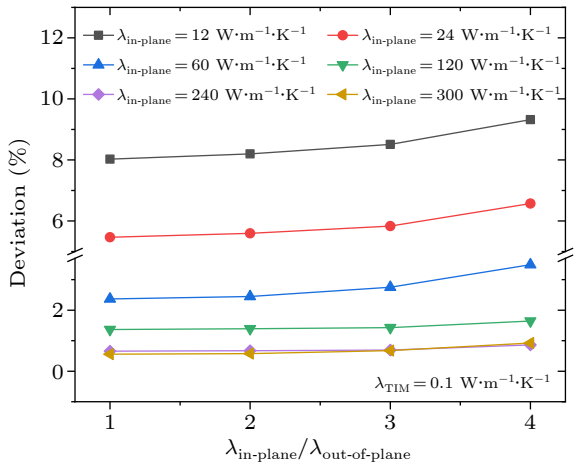

Fig. 3. Deviation in measurements of different anisotropic materials.

To further verify the numerical results, experiments are conducted on the isotropic stainless steel, aluminum and anisotropic C/SiC composite. In the experiment, the ambient temperature is fixed at 20 ℃ to analyze the influence of different λ_{TIM} on the measurement by using four different thermal insulation materials for comparison. As shown in Fig. S8, the red point in the figure represents the deviation between the numerical result and the given value. As the λ_{TIM} increases, the measured $\lambda_{\text{in-plane}}$ increases in all the materials accordingly because the heat dissipation ratio of the background thermal insulation material increases, which is consistent with the numerical results. The above results prove that the $\lambda_{\text{in-plane}}$ of 2D plain woven C/SiC composite measured via the slab module of the TPS method is reliable.

4.2 Influence of Temperature on the Anisotropic Thermal Conductivity. Figure 4 shows the measured $\lambda_{\text{in-plane}}$ of 2D plain woven C/SiC composite within the temperature range 20–900 ℃. It increases with temperature in the range 20–200 ℃ and then almost remains unchanged with the increment of temperature from 200 ℃ to 900 ℃. The measured $\lambda_{\text{in-plane}}$ is in the range of $17.8\,\text{W}\cdot\text{m}^{-1}\cdot\text{K}^{-1}$–$21.07\,\text{W}\cdot\text{m}^{-1}\cdot\text{K}^{-1}$ within the test temperature range. Since λ_{TIM} rises with temperature,[30] the deviation it brought in also increases accordingly. Thus, an expression can be obtained to reduce the influence of background thermal insulation materials. According to the λ of aluminum silicate fiberboard measured at different temperatures,[30] the deviation it brings to the thermal conductivity measurement [Fig. S8(c)] can be fitted in Eq. (2) with a correlation coefficient larger than 0.999. With the correlation, the measured $\lambda_{\text{in-plane}}$ can be modified, and the result is also presented in Fig. 4,

$$E = -3233.47\lambda_{\text{TIM}}^4 + 2145.73\lambda_{\text{TIM}}^3 - 547.56\lambda_{\text{TIM}}^2 + 94.26\lambda_{\text{TIM}} + 1.4, \tag{2}$$

where E is the deviation in slab module measurement introduced by non-ideal thermal insulation.

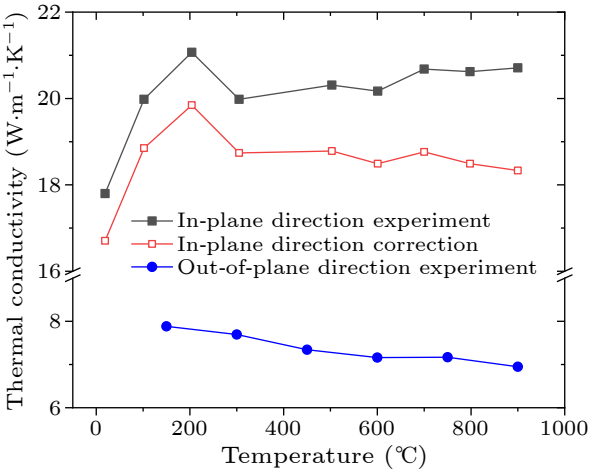

Fig. 4. Comparison of anisotropic thermal conductivity of C/SiC composite.

Figure 5 shows that the $a_{\text{out-of-plane}}$ of the 2D plain woven C/SiC composite decreases with the increment of temperature. The c_{p} of the C/SiC composite increases rapidly within the temperature below 300 ℃ and then increases linearly with temperature. The reason for the variation of c_{p} is that the molecular structure of carbon fiber is similar to that of graphite, and its Debye temperature is about 1627–1727 ℃ while the Debye temperature of the

SiC matrix is about 927–1027 ℃. The highest test temperature of 900 ℃ is lower than the Debye temperatures of carbon fiber and the SiC matrix. Thus, the specific heat capacity of carbon fiber and the SiC matrix increases with temperature within the range from room temperature to 900 ℃. As shown in Fig. 5, the thermogravimetric analysis by the STA shows that the variation in the mass ratio of the studied C/SiC composite is less than 1% within the test temperature range, which can be ignored. The $\lambda_{\text{out-of-plane}}$ of 2D C/SiC composite is determined by the measured $a_{\text{out-of-plane}}$, c_{p}, and ρ, as displayed in Fig. 4. Within the temperature range, the measured $\lambda_{\text{out-of-plane}}$ decreases from 7.89 $\text{W}\cdot\text{m}^{-1}\cdot\text{K}^{-1}$ to 6.95 $\text{W}\cdot\text{m}^{-1}\cdot\text{K}^{-1}$. The anisotropic ratio of the studied 2D plain woven C/SiC composite is within the range of 2.2 to 3.1.

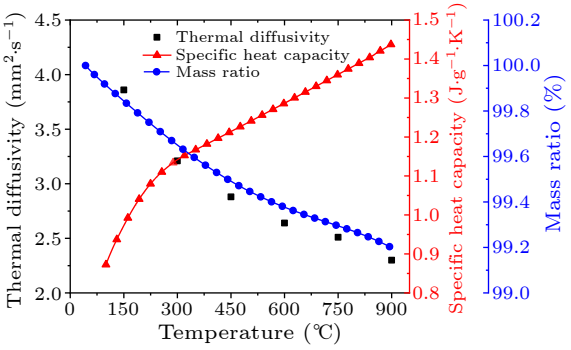

Fig. 5. Measured out-of-plane thermal diffusivity, specific heat capacity, and mass ratio of C/SiC composite.

The temperature-dependent $\lambda_{\text{anisotropic}}$ of C/SiC composite is highly related to its components. With carbon fibers and the SiC matrix, the heat transfer relies mainly on phonon heat transfer, and the lattice vibrations are intensified with temperature, which results in an increase in thermal conductivity with temperature.[31] However, as the temperature increases, the presence of different defects in the SiC matrix leads to an increase in phonon scattering and a decrease in thermal conductivity. As a result, both the transverse and longitudinal thermal conductivities of the carbon fiber increase slowly with temperature, while the thermal conductivity of SiC matrix first increases when the temperature is not higher than 100 ℃, and then decreases with temperature.[14,32] Due to the variation in thermal conductivity of the two components with temperature, the $\lambda_{\text{in-plane}}$ of the C/SiC composites increases in the range from room temperature to 200 ℃, then decreases with temperature, and tends to be essentially unchanged eventually. The measured anisotropic thermal conductivity of 2D plain woven C/SiC composite at different temperatures can be utilized for composite optimization and fine design of thermal protection systems.

5. Conclusions. In this study, the test uncertainty of a TPS slab module when measuring different isotropic and anisotropic materials is quantitatively analyzed using numerical simulation. Experiments are also conducted to validate the numerical results. The $\lambda_{\text{in-plane}}$ and $\lambda_{\text{out-of-plane}}$ of 2D plain woven C/SiC composite are measured within temperatures ranging from 20–900 ℃ using the TPS slab module and LFA method, respectively.

The $\lambda_{\text{in-plane}}$ measured using the TPS method will be overestimated due to the inconsistency between the practical heat transfer process and the theoretical assumption. With the increment of λ_{TIM}, the deviation when measuring the $\lambda_{\text{in-plane}}$ of the slab specimen increases accordingly due to increased heat loss via the background thermal insulation material. The deviation reduces swiftly as the thermal conductivity ratio of the test slab to the thermal insulation material increases. When the thermal conductivity ratio is larger than 100, the deviation will be less than 10%. To ensure that the deviation caused by the non-ideal theoretical assumption is less than 5%, the thermal conductivity ratio should be greater than 300. The anisotropic ratio of the slab material has a negligible effect on the $\lambda_{\text{in-plane}}$ measurement of the slab module. The comparison of numerical simulations with experimental measurements proves that the $\lambda_{\text{in-plane}}$ of 2D plain woven C/SiC composite measured by the slab module of the TPS method is reliable. By fitting the expression between the deviation and the λ_{TIM}, the accuracy of the measured $\lambda_{\text{in-plane}}$ of the slab specimen can be improved. Based on the numerical results, an acceptable test accuracy of TPS slab module measurement can be obtained.

The measured $\lambda_{\text{in-plane}}$ of 2D plain woven C/SiC composite increases with temperature within the ranges of 20–200 ℃, and decreases with the temperature within the range from 200 ℃ to 900 ℃. The value of the measured $\lambda_{\text{in-plane}}$ varies between 17.8 $\text{W}\cdot\text{m}^{-1}\cdot\text{K}^{-1}$–21.07 $\text{W}\cdot\text{m}^{-1}\cdot\text{K}^{-1}$. Meanwhile, both the $\lambda_{\text{out-of-plane}}$ and $a_{\text{out-of-plane}}$ decrease in the temperature range of 150–900 ℃, and the value of the $\lambda_{\text{out-of-plane}}$ is in the range of 6.95 $\text{W}\cdot\text{m}^{-1}\cdot\text{K}^{-1}$–7.89 $\text{W}\cdot\text{m}^{-1}\cdot\text{K}^{-1}$. The ratio of $\lambda_{\text{in-plane}}$ to $\lambda_{\text{out-of-plane}}$ of the 2D plain woven C/SiC composite is within the range of 2.2 to 3.1. The measured thermal conductivities are useful for composite optimization and fine design of thermal protection systems.

Acknowledgements. This work was supported by the National Natural Science Foundation of China (Grant Nos. 52276086 and 52130604), the Basic Research Program of China (Grant No. 514010303-102), and the K. C. Wong Education Foundation.

References

[1] Yin X W, Cheng L F, Zhang L T, Travitzky N, and Greil P 2017 *Int. Mater. Rev.* **62** 117

[2] Ma S H, Li Y G, Zhou J, and Zhu Z X 2023 *Chin. Phys. Lett.* **40** 084201

[3] Li X H, Yan Q Z, Mi Y Y, Han Y J, Wen X, and Ge C H 2015 *Chin. Phys. B* **24** 026103

[4] Zhang Q M 2011 *Adv. Mater. Res.* **284–286** 324

[5] Cao L Y, Liu Y S, Zhang Y H, Wang J, and Chen J 2020 *J. Eur. Ceram. Soc.* **40** 3520

[6] Naslain R 2004 *Compos. Sci. Technol.* **64** 155

[7] Zhang H, Yang Y, Liu B, and Huang Z R 2019 *Ceram. Int.* **45** 10800

[8] Stalin M, Rajaguru K, and Rangaraj L 2020 *J. Eur. Ceram. Soc.* **40** 290

[9] Caccia M, and Narciso J 2019 *Materials* **12** 2425

[10] Li J, Jiao G Q, Wang B, Yang C P, and Wang G 2014 *Chin. J. Aeronaut.* **27** 1586

[11] Zhang Y H, Liu Y S, Cao Y J, Cao L Y, Zheng X T, Wang J, Pan Y, and Wang N 2021 *Ceram. Int.* **47** 19115

[12] Zhang Y H, Liu Y S, Cao Y J, Cao L Y, Wang J, Pan Y, and Wang N 2021 *J. Am. Ceram. Soc.* **104** 645

[13] Cai Y Z, Cheng L F, Zhang H J, Yin X W, Yin H F, and Yan G Z 2019 *J. Alloys Compd.* **770** 989

[14] Xu Y J, Ren S X, and Zhang W H 2018 *Compos. Struct.* **193** 212

[15] Yang Y, Xu F, Gao X Y, and Liu G W 2016 *Mater. Design* **90** 635

[16] Dong K, Liu K, Pan L J, Gu B H, and Sun B Z 2016 *Compos. Struct.* **154** 319

[17] Gou J J, Zhang H, Dai Y J, Li S, and Tao W Q 2015 *Compos. Struct.* **125** 499

[18] Villière M, Lecointe D, Sobotka V, Boyard N, and Delaunay D 2013 *Compos. Part A: Appl. Sci. Manufact.* **46** 60

[19] Wang Y, Han T C, Liang D F, and Deng L J 2023 *Chin. Phys. Lett.* **40** 104101

[20] Lou Q and Xia M G 2023 *Chin. Phys. Lett.* **40** 094401

[21] Liu Y, Qu Z G, Guo J, and Zhao X M 2019 *Int. J. Heat Mass Transfer* **140** 410

[22] Gou J J, Dai Y J, Li S G, and Tao W Q 2015 *Int. J. Heat Mass Transfer* **91** 829

[23] Li S S, Tong X Y, Yao L J, and Li B 2012 *Adv. Mater. Res.* **460** 342

[24] Choi H I, Zhu F Y, Lim H, and Yun G J 2019 *Compos. Part B: Eng.* **177** 107375

[25] ISO 8894-1:2010 Refractory Materials—Determination of Thermal Conductivity Part 1: Hot-Wire Methods (Cross-Array and Resistance Thermometer) 2021

[26] Zhang H, Jin Y, Gu W, Li Z Y, and Tao W Q 2013 *Prog. Comput. Fluid Dyn.* **13** 191

[27] Zhang H, Wu K F, Xiao G M, Du X Y, and Tang G H 2021 *Compos. Struct.* **267** 113870

[28] He Y 2005 *Thermochim. Acta* **436** 122

[29] Yan H L, Yan J L, and Zhao G 2019 *Chin. Phys. B* **28** 114401

[30] Zhang H, Shang C Y, and Tang G H 2022 *Int. J Therm. Sci.* **171** 107261

[31] Jiang J H, Lu S, and Chen J 2023 *Chin. Phys. Lett.* **40** 096301

[32] Sun Z, Shan Z D, and Shao T M 2021 *Int. J. Heat Mass Transfer* **170** 120973